

# Two-photon pumped exciton-polariton condensation

N. Landau<sup>1✉</sup>, D. Panna<sup>1</sup>, S. Brodbeck<sup>2</sup>, C. Schneider<sup>3</sup>, S. Höfling<sup>2</sup> and A. Hayat<sup>1✉</sup>

The discovery of Two-Photon Absorption (TPA)<sup>1,2</sup> has led to remarkable advances in fields such as fluorescence microscopy<sup>3</sup> and optical data storage<sup>4</sup>. Simultaneously, the search for reliable and efficient terahertz (THz) radiation sources for numerous applications in communications, biosensing, and security has attracted considerable interest in the scientific community<sup>5</sup>; however, to date, their efficiency remains limited. Recently, it has been proposed that highly efficient THz emission can be achieved by TPA into a quantum condensate of strongly-coupled light-matter exciton-polaritons<sup>6,7,8,9,10</sup> through the bosonic final state stimulation effect<sup>11</sup>. Here we report the first experimental observation of two-photon excitation of such a polariton condensate, demonstrated by angle-resolved photoluminescence in a GaAs-based microcavity. TPA is evidenced in the quadratic dependence of the emission on pump power below and above the condensation threshold. Second-harmonic generation (SHG) is ruled out by observing both this threshold behavior and a lack of dependence of the emission peak energy on the pump photon energy. Our results pave the way towards the realization of a polariton-based THz laser source and shed new light on collective states of matter.

Efficient radiation sources in the terahertz (THz) region of the electromagnetic spectrum are highly sought after for many technological applications<sup>5</sup>; however, the quest for finding them presents a fundamental physical challenge, now widely referred to as “the THz gap”<sup>12</sup>. Spontaneous emission rates of THz photons are typically many orders of magnitude slower than competing nonradiative carrier decay rates<sup>13,14</sup>. Numerous techniques have been employed attempting to overcome this issue. Generating THz radiation based on photoconductive and optical mixing techniques are well-established methods<sup>15,16,17,18</sup>, with another prominent direction being THz quantum cascade lasers<sup>19,20,21</sup>; however, all these THz sources still exhibit relatively low quantum efficiency. A recent work<sup>11</sup> has predicted that orders of magnitude increased efficiency of the THz emission can be realized in a strongly-coupled microcavity operating in the polariton condensation regime. This can be achieved by two-photon absorption (TPA) into the 2p “dark” exciton state in the cavity-embedded quantum well (QW), such that a subsequent THz transition to the 1s-exciton-based lower polariton (LP) ground state becomes stimulated when feeding a polariton condensate. Embedding the

---

<sup>1</sup>Department of Electrical Engineering, Technion, Haifa 32000, Israel. <sup>2</sup>Technische Physik, Universität Würzburg, Am Hubland, D-97074 Würzburg, Germany. <sup>3</sup>Institute of Physics, University of Oldenburg, 26129 Oldenburg, Germany. ✉e-mail address: [nlandau@campus.technion.ac.il](mailto:nlandau@campus.technion.ac.il) ; [alex.hayat@ee.technion.ac.il](mailto:alex.hayat@ee.technion.ac.il)

structure within a supporting THz cavity could then lead to a double bosonic stimulation effect, where stimulation is provided by the macroscopic occupation of both the polariton condensate and THz cavity mode, potentially increasing the THz lasing efficiency to unprecedented levels.

Lately, significant efforts have been made towards the implementation of such a scheme, peaking with the demonstration of TPA-based excitation of non-condensed polaritons<sup>22,23,24,25,26</sup>. However, condensation via TPA was not achieved previously due to challenges imposed by the required conditions: on the one hand, the condensation process calls for extremely high intensities injecting large carrier densities by TPA, while on the other, low pulse repetition rates are necessary to allow cool down in-between pulses<sup>27</sup>, all while still maintaining strong light-matter coupling in a condensate-supporting structure.

Here we demonstrate two-photon pumped polariton condensation, achieved by TPA-based excitation at extremely high intensities and low repetition rates. Our pump conditions enable reaching the threshold density via TPA and establishing condensation without breaking the strong light-matter coupling. We show this in a planar GaAs-based microcavity, by pumping with ultrafast pulses at energies near half the exciton levels. The resulting photoluminescence (PL) from the LP ground state exhibits a clear intensity threshold as a function of increased TPA intensity, coinciding with an interaction-induced blueshift and a spectral linewidth narrowing, characteristic of the transition from a polariton thermal distribution to polariton condensation. The emission is found to depend quadratically on pump power below and above the condensation threshold, as expected for a TPA process. The existence of a threshold rules out second-harmonic generation (SHG) as the reason for the quadratic dependence, and we verify this by scanning the pump photon energy and observing a lack of dependence of the emission peak energy.

In our experiments (see Methods), the output of a femtosecond-pulsed laser was tuned close to half the resonance energy of the 2p exciton state in our sample – at  $E_{\text{pump}} \cong 800$  meV (Fig. 1). Optical selection rules around  $k_{\parallel} = 0$  dictate that in such a TPA process, only “dark” states which are dipole-forbidden from directly coupling to light can be excited<sup>1,28</sup>. Recent

studies have shown that some direct two-photon injection of 1s "bright" excitons is possible in GaAs due to valence-band mixing effects at finite in-plane momenta<sup>24,25</sup>. However, since the strength of this mixing should be very weak for typical photonic wavenumbers, we expect the dominant absorption channel in our excitation scheme to have been the 2p "dark" exciton. Eventually, the predicted 2p-to-LP THz photon emission as well as, in principle, phonon-assisted relaxation and polariton-polariton scattering (Fig. 1), lead to the macroscopic occupation of the LP ground state and polariton condensation. Contrary to previously suggested inter-polariton (upper to lower polariton) stimulated THz transitions<sup>29</sup>, which are parity-forbidden and thus require upper polariton (UP) hybridization using an externally-applied electric field, the intraband THz radiative decay from the 2p state to the 1s-exciton-based LP is dipole-allowed<sup>30</sup>.

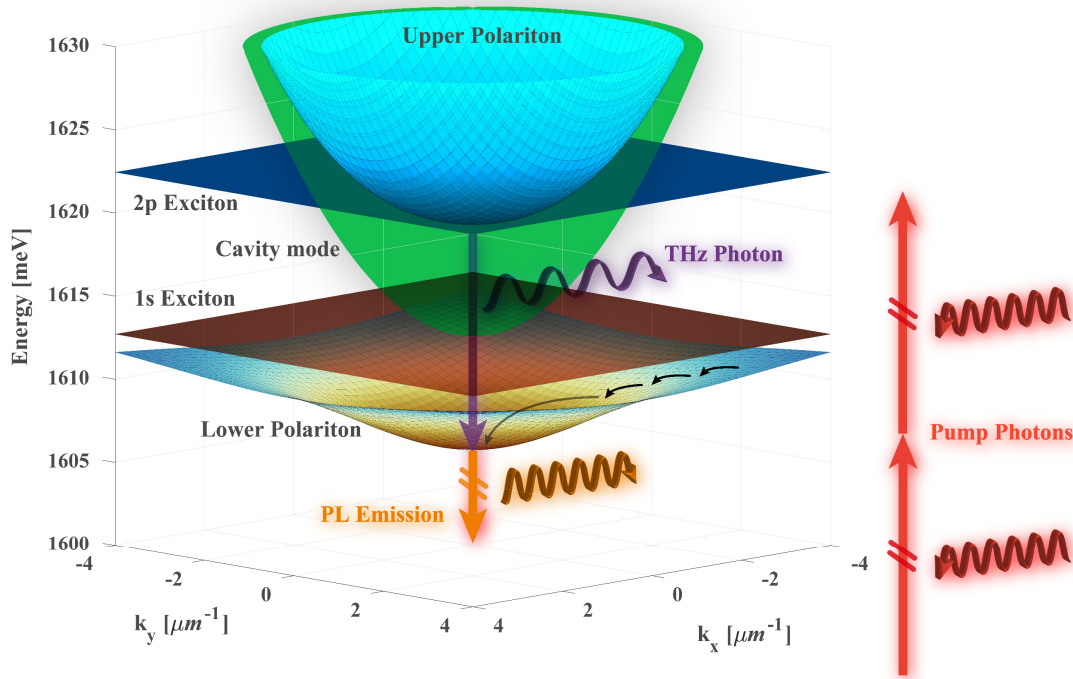


**Figure 1 | Calculated in-plane dispersion relations and two-photon pumping scheme.** Schematic of the in-plane polariton dispersion relations calculated at a 1s exciton-cavity detuning energy of  $\Delta \cong 0 \text{ meV}$ , showing the lower and upper polariton branches, as well as the 2p exciton [dark blue], 1s exciton [brown], and cavity photon mode [green] dispersions. The pump photon energy [red] is approximately half that of the exciton states; The LP PL [orange] and possible intraband THz photon [purple] emissions are depicted as well, along with other possible phonon-polariton and polariton-polariton scattering mechanisms on the LP branch [small black arrows]. Photon energies are not drawn to scale, as indicated by the double-diagonal lines on the arrows.

In our sample, we further exclude excitation of Light-Hole (LH) exciton states as these lie  $\sim 35$  meV higher than the discussed Heavy-Hole (HH) exciton states, which is greater than both the LP-UP splitting and the spectral region covered by our pump laser.

PL from our sample was collected from the central area of the two-photon pump spot and far-field analysis was then performed for various 1s exciton-cavity detuning energies  $\Delta$ . Fig. 2 shows our results for the angle-resolved PL measurements at a slightly negative 1s exciton-cavity detuning energy of  $\Delta \cong -4$  meV, and for different TPA powers. Superimposed on the plots are the calculated in-plane dispersions of the type shown in Fig. 1, determined using an appropriate coupled oscillator model<sup>31</sup> fitting our sample parameters (see Methods).

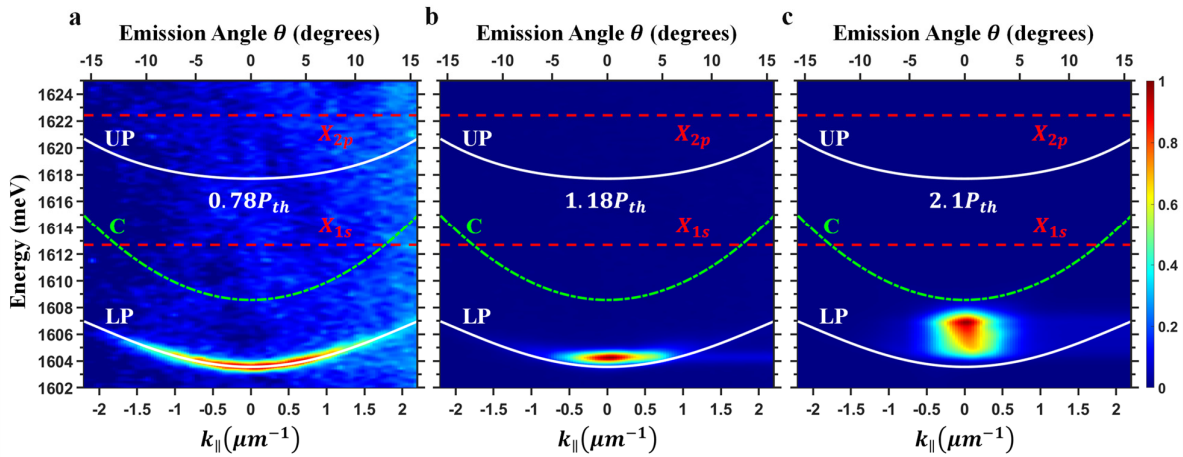


**Figure 2 | Angle-resolved PL at a 1s exciton-cavity detuning of  $\Delta \cong -4$  meV, measured at 6K for different TPA powers.** The PL in each panel is normalized and plotted in a linear color scale, with the color code indicated on the right. The lines represent the calculated LP and UP (white solid), cavity photon mode C (green dashed-dotted), and 1s ( $X_{1s}$ ) and 2p ( $X_{2p}$ ) exciton (red dashed) in-plane dispersions. **a**, Below threshold, the emission is broadly distributed in momentum and energy owing to thermally-distributed LPs. **b**, Slightly above the condensation threshold, the emission narrows spectrally and shrinks to within a small angular range of  $\pm \sim 3^\circ$ , originating from slightly blueshifted condensed polaritons around  $k_{||} = 0$ . **c**, Above threshold, the emission coming from further blueshifted condensed polaritons is smeared due to the time-integrated nature of the measurement; Horizontal axes in each panel display the in-plane momentum  $k_{||}$  (bottom) and corresponding emission angle  $\theta$  (top).

For TPA powers below the condensation threshold, emission from thermally-distributed polaritons on the LP branch is observed, as it is exclusively populated at low temperatures (Fig. 2a). At an increased power slightly above threshold, a transition appears from the broad-angle thermally-populated LP branch to a narrow and slightly blueshifted state (Fig. 2b). As has previously been established for a one-photon excitation scheme<sup>32</sup>, the above transition is associated with the build-up of a polariton condensate<sup>33,34</sup>. Increasing the TPA

power further above threshold, the emission originates from a now further-blueshifted condensate (Fig. 2c). This emission is slightly smeared to lower energies due to the fact that the polariton density changes in time following the ultrashort TPA pulse, so that in the time-integrated image (Fig. 2c), the blueshift temporal decay appears simultaneously with the peak of the blueshifted state.

To confirm the transition to a polariton condensate from the angle-resolved images, the evolution of several PL characteristics with increasing TPA powers was extracted.

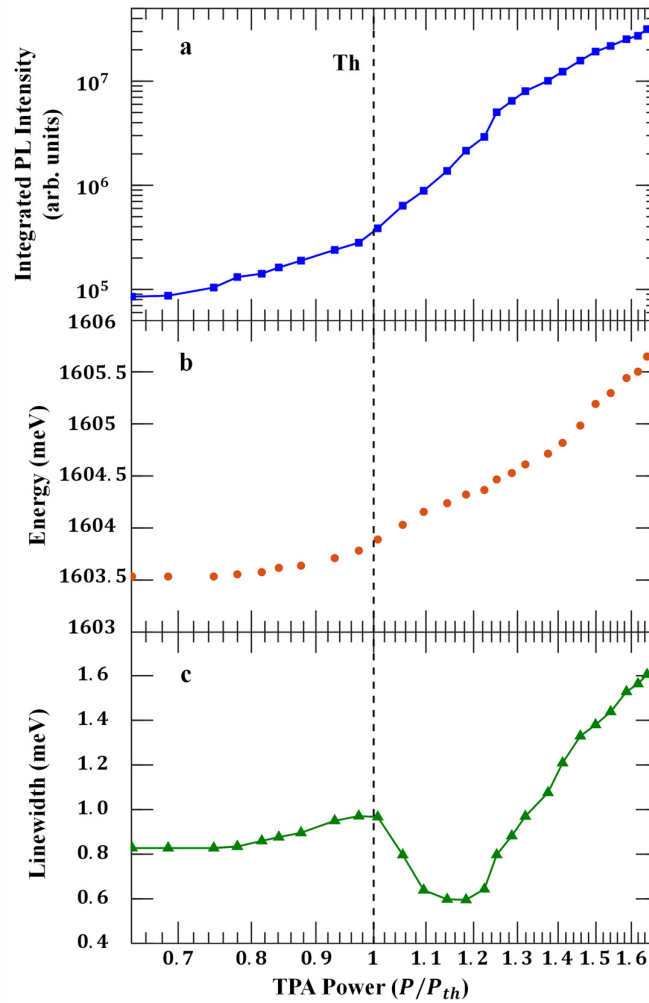


**Figure 3 | Dependence of PL characteristics on the TPA power ( $P/P_{th}$ , logscale), at  $\Delta \cong -4\text{meV}$ .** **a**, the integrated PL intensity (arb. units, logscale) within in-plane momenta  $|k_{\parallel}| \leq 0.35 \mu\text{m}^{-1}$ . The quadratic dependence below threshold strongly steepens at the condensation threshold. **b**, the PL peak energy (in meV) within the same in-plane momenta window. Being roughly constant at the LP ground state energy for lower powers, it continuously blueshifts with increasing power starting from slightly below threshold, due to self-interactions of an increasing polariton density<sup>35,36</sup>. **c**, the PL linewidth (FWHM, in meV). A clear spectral narrowing at threshold corresponds to increased temporal coherence, and the broadening at larger powers is attributed to density fluctuations and polariton-polariton interactions<sup>37</sup>; The vertical dashed line across all panels indicates the condensation threshold.

Fig. 3a shows the integrated PL intensity at a 1s exciton-cavity detuning of  $\Delta \cong -4 \text{ meV}$  as a function of the TPA power, where only low in-plane momenta ( $|k_{\parallel}| \leq 0.35 \mu\text{m}^{-1}$ ) has been considered. Below the condensation threshold, in the thermal regime, the integrated PL intensity increases quadratically with the TPA power (see Fig. 4a), until it abruptly steepens around threshold. This abrupt change occurs at a TPA power similar to the transition observed in the time-integrated image (Fig. 2b). Tracking the dependence of the PL peak energy on the TPA power, a small blueshift is observed starting from slightly below the marked threshold, as shown in Fig. 3b. In the thermal regime, the emission peak energy remains roughly constant at the LP ground state energy of  $\sim 1603.6 \text{ meV}$ . Closer to the marked threshold, this peak begins to continuously blueshift with increasing TPA power, owing to the enhanced self-interactions of an increasing polariton density<sup>35,36</sup>. This blueshift is found to be approximately quadratic in pump power for this regime and thus linear in injected population density, as expected for a polariton-polariton interaction-based mechanism following TPA. It further constitutes an important indicator for the presence of a self-interacting polariton condensate, and its total magnitude added to the sub-threshold LP ground state energy remains lower than the Rabi splitting. Examining the evolution of the PL spectral linewidth with increasing TPA powers (Fig. 3c), a very gradual increase of its FWHM bandwidth is initially observed, followed by a sharp narrowing around the condensation threshold down to about two thirds of the value at the thermal regime. This spectral narrowing corresponds to the increased temporal coherence of the condensed state. Increasing the excitation further above the threshold power, the observed linewidth starts increasing continuously due to density fluctuations and polariton-polariton interactions<sup>37</sup>, in good agreement with previous observations on one-photon pumped condensation<sup>32</sup>.

To further verify condensation in our sample, we have performed the same measurements at two different energy detunings of  $\Delta \approx 0$  meV and  $\Delta \approx 4.5$  meV between the 1s exciton and cavity mode, and similar characteristic behaviours were observed. All three detunings lie within the previously determined range for establishing polariton condensation in a GaAs-based microcavity<sup>38</sup>. To confirm the two-photon nature of the excitation, Fig. 4a shows the log-scale input-output curves for two of these cases and for an extended TPA power range. Power-law fits below and above each threshold region are also presented. The fitted values for the slopes at each detuning all show good agreement with a power-of-two input-output dependence.

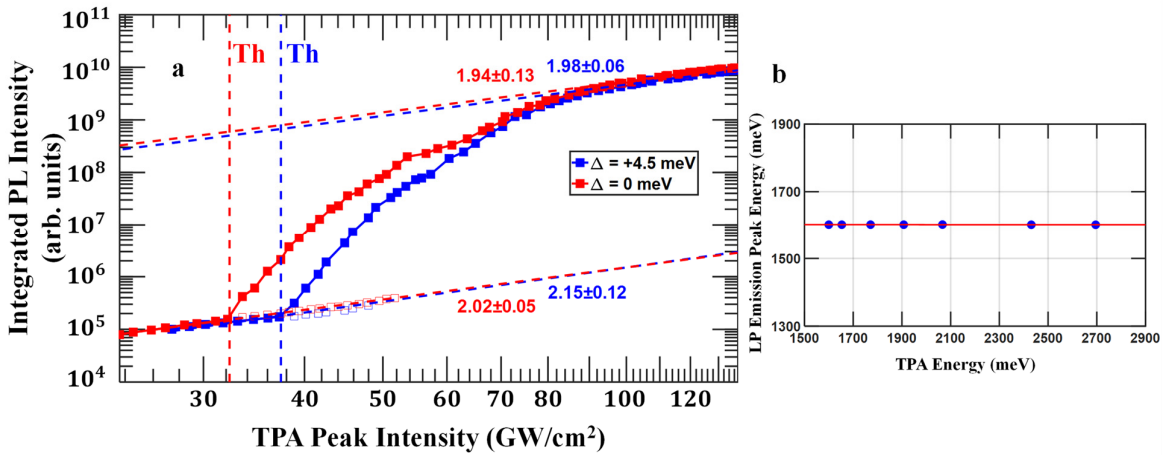


**Figure 4 | Two-photon pumped condensation at different detunings and characterization of the TPA process.** **a**, Integrated PL intensity (logscale, arb. units) vs. TPA peak intensity (logscale, in  $\text{GW}/\text{cm}^2$ ) for two detunings of  $\Delta \approx 0$  meV (red line and squares) and  $\Delta \approx +4.5$  meV (blue line and squares). Vertical dashed colored lines mark the condensation threshold in each case, of  $\sim 32.3 \text{GW}/\text{cm}^2$  and  $\sim 37.4 \text{GW}/\text{cm}^2$  respectively. Diagonal dashed colored lines are power-law fits to  $y = a \cdot x^b$ , where the values of  $b$  are  $2.02 \pm 0.05$  and  $2.15 \pm 0.12$  below threshold, for  $\Delta \approx 0$  meV and  $\Delta \approx +4.5$  meV respectively, and  $1.94 \pm 0.13$  and  $1.98 \pm 0.06$  above threshold for the same, all in good agreement with a power-of-two input-output dependence, as expected for a TPA process. **b**, LP emission peak energy (in meV) vs. TPA pump photon energy (in meV). Blue circles are recorded data and red line is a linear fit showing that effectively no dependence of the emission peak energy is observed when scanning the pump energy across a wide two-photon spectral range.

The observed threshold behaviour of the emission rules out SHG as the reason for the power-of-two dependence, and to further confirm this we have scanned the pump two-photon energy and recorded the resulting LP emission peak energy. For a pump-induced SHG process, the emission peak energy is expected to shift spectrally along with the scanned pump two-photon energy. As Fig. 4b clearly reflects no such dependence of the emission peak

energy on the pump two-photon energy, and as mentioned, the emission shows a clear condensation threshold, SHG is ruled out as a cause for the observed power-of-two dependence.

In conclusion, we observe two-photon pumped condensation of exciton-polaritons. The angle-resolved photoluminescence from the LP ground state in our planar GaAs-based microcavity exhibits a clear, detuning-dependent intensity threshold with increasing TPA peak intensities, at which the onset of a steep nonlinearity in the input-output curve, an interaction-induced blueshift of the central emission peak, and a sharp spectral narrowing of this peak corresponding to an increased temporal coherence, are all simultaneously observed, as expected for a transition to a polariton condensate<sup>38</sup>. The log-scale input-output curves for two different detunings exhibit a power-of-two dependence below and above the threshold region, confirming the TPA excitation scheme. For a pump-induced SHG process, no such threshold behaviour is expected. The emission peak energy is further expected to shift for such a process when scanning the pump two-photon energy, in contradiction to our observations (Fig. 4b). The above results present a platform for realizing a polariton-based stimulated THz radiation source<sup>11</sup> and shed new light on nonlinear-optical excitation of dark states and quantum condensates.

## Methods

**Microcavity structure.** Our sample consists of a  $\lambda/2$  AIAs intracavity layer embedded between two distributed Bragg reflector (DBR) structures of  $\text{Al}_{0.2}\text{Ga}_{0.8}\text{As}/\text{AIAs}$ , where the upper (lower) DBR structure consists of 23 (27) alternating layers of  $\text{Al}_{0.2}\text{Ga}_{0.8}\text{As}$  and AIAs, giving a cavity Q-factor of  $\sim 5000$ . Three stacks of four 7 nm GaAs QWs with 4 nm AIAs barriers are placed at the three antinode positions of the confined microcavity mode, and the resulting normal-mode splitting with the QW 1s HH1 exciton state is measured to be  $\sim 13.6$  meV, with a clear anti-crossing of their reflectivity dips observed as the 1s exciton-cavity detuning tends to zero. The LP and UP resonances at Strong Coupling (SC) are found to be at  $\sim 1605.9$  meV and  $\sim 1619.5$  meV, respectively. The sample thickness is tapered across along one axis to allow access to different 1s exciton-cavity detuning energies by impinging different spots along that axis. Condensation of lower polaritons is also evidenced in our sample under nonresonant one-photon pulsed excitation at different 1s exciton-cavity detuning energies. Figures and further details on the sample characterization can be found in a previous publication<sup>39</sup>.

**Experimental Setup.** In our experimental setup, the sample was held in a closed-cycle liquid helium-flow cryostat at  $\sim 6$  K. For our TPA spectroscopy experiment, the output of an Optical-Parametric Amplifier (OPA) pumped by a regenerative-amplifier Ti:Sapph femtosecond-pulsed laser with a repetition rate of 1 KHz at 1550 meV was used and was tuned close to half the resonance energy of the LP ground state and the QW 2p HH1 exciton state in our sample – at roughly  $E_{\text{pump}} \cong 800$  meV. An automated variable neutral density filter was then used to controllably attenuate the  $\sim 70$  femtosecond pulsed pump beam, and a premium longpass filter was used to suppress any possible residual higher harmonics from the OPA. The pump was then focused onto the sample to an elliptically shaped spot of area  $\sim 53000 \mu\text{m}^2$ , at an angle of  $\sim 30^\circ$  from normal incidence. The resulting PL was collected from the central area of the two-photon pump spot using an infinity-corrected microscope objective with a numerical aperture  $\text{NA} = 0.42$ . To investigate the emission in the far-field, the objective Fourier plane was imaged onto the entrance slit of a spectrometer using a set of relaying optics, and detected using a thermoelectric-cooled Electron-Multiplying CCD camera. Measurements were then taken for several energy detunings between the cavity mode and QW 1s HH1 exciton, separated by more than the pump spot-limited detuning resolution of  $\sim 2$  meV.

## References

1. Göppert-Mayer, M. Über elementarakte mit zwei quantensprüngen. *Annalen der Physik* **401**, 273-294 (1931).
2. Kaiser, W., & Garrett, C. G. B. Two-photon excitation in  $\text{CaF}_2:\text{Eu}^{2+}$ . *Phys. Rev. Lett.* **7**, 229 (1961).
3. Denk, W., Strickler, J. H., & Webb, W. W. Two-photon laser scanning fluorescence microscopy. *Science* **248**, 73-76 (1990).
4. Parthenopoulos, D. A., & Rentzepis, P. M. Three-dimensional optical storage memory. *Science* **245**, 843-845 (1989).
5. Tonouchi, M. Cutting-edge terahertz technology. *Nat. Photonics* **1**, 97-105 (2007).
6. Imamoglu, A., Ram, R. J., Pau, S., & Yamamoto, Y. Nonequilibrium condensates and lasers without inversion: Exciton-polariton lasers. *Phys. Rev. A* **53**, 4250 (1996).

- 
7. Deng, H., Weihs, G., Santori, C., Bloch, J., & Yamamoto, Y. Condensation of semiconductor microcavity exciton polaritons. *Science* **298**, 199-202 (2002).
  8. Deng, H., Weihs, G., Snoke, D., Bloch, J., & Yamamoto, Y. Polariton lasing vs. photon lasing in a semiconductor microcavity. *Proc. Natl. Acad. Sci. USA* **100**, 15318-15323 (2003).
  9. Kasprzak, J. et. al. Bose–Einstein condensation of exciton polaritons. *Nature* **443**, 409-414 (2006).
  10. Schneider, C. et. al. An electrically pumped polariton laser. *Nature* **497**, 348-352 (2013).
  11. Kavokin, A. V., Shelykh, I. A., Taylor, T., & Glazov, M. M. Vertical cavity surface emitting terahertz laser. *Phys. Rev. Lett.* **108**, 197401 (2012).
  12. Davies, G., & Linfield, E. Bridging the terahertz gap. *Phys. world* **17**, 37 (2004).
  13. Duc, H. T., Vu, Q. T., Meier, T., Haug, H., & Koch, S. W. Temporal decay of coherently optically injected charge and spin currents due to carrier–LO-phonon and carrier-carrier scattering. *Phys. Rev. B* **74**, 165328 (2006).
  14. Doan, T. D., Cao, H. T., Thoai, D. T., & Haug, H. Condensation kinetics of microcavity polaritons with scattering by phonons and polaritons. *Phys. Rev. B* **72**, 085301 (2005).
  15. Fattinger, C., & Grischkowsky, D. Terahertz beams. *Appl. Phys. Lett.* **54**, 490-492 (1989).
  16. Brown, E. R., McIntosh, K. A., Nichols, K. B., & Dennis, C. L. Photomixing up to 3.8 THz in low-temperature-grown GaAs. *Appl. Phys. Lett.* **66**, 285-287 (1995).
  17. Kawase, K., Sato, M., Taniuchi, T., & Ito, H. Coherent tunable THz-wave generation from LiNbO<sub>3</sub> with monolithic grating coupler. *Appl. Phys. Lett.* **68**, 2483-2485 (1996).
  18. Vodopyanov, K. L. et. al. Terahertz-wave generation in quasi-phase-matched GaAs. *Appl. Phys. Lett.* **89**, 141119 (2006).
  19. Faist, J. et. al. Quantum cascade laser. *Science* **264**, 553-556 (1994).
  20. Williams, B. S. Terahertz quantum-cascade lasers. *Nat. Photonics* **1**, 517-525 (2007).
  21. Belkin, M. A. et. al. Terahertz quantum-cascade-laser source based on intracavity difference-frequency generation. *Nat. Photonics* **1**, 288-292 (2007).
  22. Leménager, G. et. al. Two-photon injection of polaritons in semiconductor microstructures. *Opt. Lett.* **39**, 307-310 (2014).
  23. Schmutzler, J. et. al. Nonlinear spectroscopy of exciton-polaritons in a GaAs-based microcavity. *Phys. Rev. B* **90**, 075103 (2014).
  24. Steger, M., Gautham, C., Snoke, D. W., Pfeiffer, L., & West, K. Slow reflection and two-photon generation of microcavity exciton–polaritons. *Optica* **2**, 1-5 (2015).
  25. Gautham, C., Steger, M., Snoke, D., West, K., & Pfeiffer, L. Time-resolved two-photon excitation of long-lifetime polaritons. *Optica* **4**, 118-123 (2017).
  26. Lundt, N. et. al. Optical valley Hall effect for highly valley-coherent exciton-polaritons in an atomically thin semiconductor. *Nat. Nanotechnology* **14**, 770-775 (2019).
  27. Schmidt, D. et. al. Tracking dark excitons with exciton polaritons in semiconductor microcavities. *Phys. Rev. Lett.* **122**, 047403 (2019).

- 
28. Tai, K., Mysyrowicz, A., Fischer, R. J., Slusher, R. E., & Cho, A. Y. Two-photon absorption spectroscopy in GaAs quantum wells. *Phys. Rev. Lett.* **62**, 1784 (1989).
29. Kavokin, K. V. et. al. Stimulated emission of terahertz radiation by exciton-polariton lasers. *Appl. Phys. Lett.* **97**, 201111 (2010).
30. Slavcheva, G., & Kavokin, A. V. Polarization selection rules in exciton-based terahertz lasers. *Phys. Rev. B* **88**, 085321 (2013).
31. Pau, S., Björk, G., Jacobson, J., Cao, H., & Yamamoto, Y. Microcavity exciton-polariton splitting in the linear regime. *Phys. Rev. B* **51**, 14437 (1995).
32. Tempel, J. S. et. al. Characterization of two-threshold behavior of the emission from a GaAs microcavity. *Phys. Rev. B* **85**, 075318 (2012).
33. Wouters, M., Carusotto, I., & Ciuti, C. Spatial and spectral shape of inhomogeneous nonequilibrium exciton-polariton condensates. *Phys. Rev. B* **77**, 115340 (2008).
34. Maragkou, M., Grundy, A. J. D., Ostatnický, T., & Lagoudakis, P. G. Longitudinal optical phonon assisted polariton laser. *Appl. Phys. Lett.* **97**, 111110 (2010).
35. Richard, M. et. al. Experimental evidence for nonequilibrium Bose condensation of exciton polaritons. *Phys. Rev. B* **72**, 201301 (2005).
36. Ciuti, C., Savona, V., Piermarocchi, C., Quattropani, A., & Schwendimann, P. Role of the exchange of carriers in elastic exciton-exciton scattering in quantum wells. *Phys. Rev. B* **58**, 7926 (1998).
37. Porras, D., & Tejedor, C. Linewidth of a polariton laser: Theoretical analysis of self-interaction effects. *Phys. Rev. B* **67**, 161310 (2003).
38. Schmutzler, J. et. al. Determination of operating parameters for a GaAs-based polariton laser. *Appl. Phys. Lett.* **102**, 081115 (2013).
39. Panna, D.\* , Landau, N.\* et. al. Ultrafast Manipulation of a Strongly Coupled Light–Matter System by a Giant ac Stark Effect. *ACS Photonics* **6**, 3076 (2019).